

Production of χ_{c1} in e^+e^- collision

Tong Liu on behalf of the BESIII collaboration

Fudan University, Shanghai, China.

e-mail: liutong2016@ihep.ac.cn

Received 15 January 2022; accepted 15 March 2022

The direct production of the charmonium state χ_{c1} in electron positron annihilation is searched by using e^+e^- collision data at four center-of-mass energies, 3.5080, 3.5097, 3.5104 and 3.5146 GeV collected with the BESIII detector at the BEPC-II collider. By combining the 4 data samples, the χ_{c1} signal is observed with a significance of 5.1σ . An interference pattern between the signal process of $e^+e^- \rightarrow \chi_{c1} \rightarrow \gamma J/\psi \rightarrow \gamma\mu^+\mu^-$ and the background process of $e^+e^- \rightarrow \gamma_{\text{ISR}} J/\psi \rightarrow \gamma_{\text{ISR}}\mu^+\mu^-$ is identified. This is the first observation of a C -even state produced directly in e^+e^- annihilation. At 68.3% confidence level, the electronic width of χ_{c1} is determined to be $\Gamma_{ee} = (0.12^{+0.13}_{-0.08})$ eV.

Keywords: e^+e^- annihilation; charmonium; electronic width; BESIII; two-photon process.

DOI: <https://doi.org/10.31349/SuplRevMexFis.3.0308059>

1. Introduction

Up to now, the direct production of resonances in electron positron annihilation has only been observed for states with quantum numbers $J^{PC} = 1^{--}$. The quantum numbers J , P , C , denote the total angular momentum, the parity and the charge-conjugation, respectively. The direct production of the C -even states, such as the axial vector charmonium state χ_{c1} could happen through two-photon or neutral current. Such processes have been considered theoretically [1] a long time already, and searched for experimentally at the VEPP-2M [2-4], VEPP-2000 [5-7], BEPC-II [8] and KEKB [9] colliders. At the SND experiment, the process of $e^+e^- \rightarrow f_1(1285)$ was studied, the significance was found to be 2.5σ [7]. Also, the process of $\gamma\gamma^* \rightarrow X(3872)$ was studied by the Belle experiment, and a significance of 3.2σ was reported [9]. Due to the smallness of the production cross section and the limited statistics, by now no observation has been reported.

The production rate is proportional to the electronic width of the states (Γ_{ee}). For the χ_{c1} state, there are several theoretical predictions. Based on unitarity, the lower limit of the Γ_{ee} of χ_{c1} is 0.044 eV [1]. Using the vector meson dominance model [10] and the non-perturbative Quantum Chromodynamics framework [11], two calculations estimated the Γ_{ee} to be at the 0.1 eV level. Recently, following the strategy used in Ref. [1], the authors of Ref. [12] predict $\Gamma_{ee} = 0.43$ eV or 0.41 eV depending on whether the contribution of neutral current is included or not. In the calculation, the authors also consider the interference between the process of $e^+e^- \rightarrow \chi_{c1} \rightarrow \gamma J/\psi \rightarrow \gamma\mu^+\mu^-$, and the processes of $e^+e^- \rightarrow \gamma_{\text{ISR}} J/\psi \rightarrow \gamma_{\text{ISR}}\mu^+\mu^-$ and $e^+e^- \rightarrow \gamma_{\text{ISR}}\mu^+\mu^-$. The interference effect distort the total cross section line-shape dramatically, as shown in Fig. 1.

The BESIII detector [13] records symmetric e^+e^- collisions provided by the BEPC-II storage ring [14], which operates with a peak luminosity of $1 \times 10^{33} \text{ cm}^{-2}\text{s}^{-1}$ in the

center-of-mass energy range from 2.0 to 5.0 GeV. The excellent performance of BEPC-II/BESIII offers a good opportunity to search for the process $e^+e^- \rightarrow \chi_{c1}$.

2. Data samples and analysis strategy

The χ_{c1} scan samples are collected at four c.m. energies (\sqrt{s}) around the χ_{c1} mass region (3.5080, 3.5097, 3.5104, and 3.5146 GeV, referred to as χ_{c1} scan sample). The c.m. energies and the beam-energy spread are measured with a beam energy measurement system (BEMS) [15]. The integrated luminosity of each data sample is measured by using large angle Bhabha events. The total integrated luminosity of the four data samples is amounts to 446 pb^{-1} , as listed in Table II. According to the calculation in Ref. [12], if the interference is taken into account, the excess at the first and the second points should be resolved. The χ_{c1} contribution should be close to zero at the third point, while a reduction at the fourth point is expected. If there are no interference contributions considered, the excess of events at the third point should be the largest.

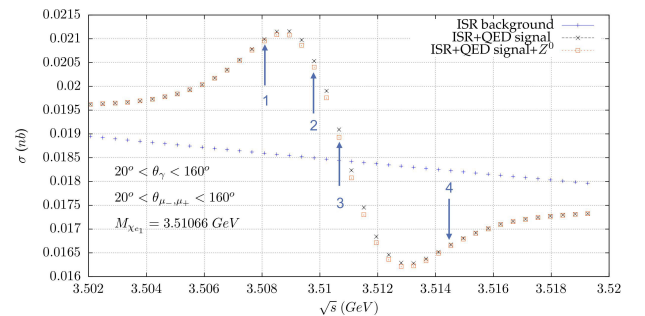


FIGURE 1. Differential cross section predicted in Ref. [12] for the background process $e^+e^- \rightarrow \gamma_{\text{ISR}} J/\psi \rightarrow \gamma_{\text{ISR}}\mu^+\mu^-$ (blue points) and for the total cross section of $e^+e^- \rightarrow \gamma\mu^+\mu^-$ including the χ_{c1} signal contribution (red points). The blue arrows indicate the location of the BESIII data samples.

Simulated samples produced with a GEANT4-based [16] Monte Carlo (MC) package, which includes the geometric description of the BESIII detector and the detector response, are used to determine the detection efficiencies and to estimate the background contributions. The PHOKHARA, PHOKHARA_WEB event generator with beam-energy spread included as an input parameter is used to describe the process of $e^+e^- \rightarrow \gamma\mu^+\mu^-$ including both signal and background contributions. Inclusive MC simulated events are used to study the non- $\gamma\mu^+\mu^-$ background events at the control samples [18].

In this study, the χ_{c1} is reconstructed via its radiative decay $\chi_{c1} \rightarrow \gamma J/\psi$ with the subsequent decay $J/\psi \rightarrow \mu^+\mu^-$. The irreducible background is $e^+e^- (\rightarrow \gamma_{\text{ISR}} J/\psi) \rightarrow \gamma_{\text{ISR}} \mu^+\mu^-$ since the processes have the same final state. We firstly validate the description of the irreducible background from MC simulation using control data samples. If the description is good, the excess (reduction) of events beyond background, *i.e.* the signal process $e^+e^- \rightarrow \chi_{c1}$, will be searched for using the χ_{c1} scan sample. The interference pattern will be studied by combining all the data samples around the χ_{c1} mass region.

The validation of the description of the irreducible ISR background is performed by applying the same study at the samples taken at $\sqrt{s} = 3.773$ and 4.178 GeV with high statistics (3 fb^{-1} each), and the samples taken at $\sqrt{s} = 3.581$ and 3.670 GeV with lower statistics (85 pb^{-1} each).

3. Search for $e^+e^- \rightarrow \chi_{c1}$

By using the method as described in Ref. [18], all the final state particles are reconstructed. Muon tracks are identified with the deposited energy in the Electromagnetic Calorimeter (EMC). A vertex fit is performed to the charged tracks and a four constraint (4C) kinematic fit is performed to all the final particles. The photon with best 4C fit quality is chosen as the

best photon candidate, whose polar angle is required to be $|\cos\theta_\gamma| < 0.80$ to increase the signal-to-background ratio as the distribution from the dominant background events from the ISR process peaks at small angles.

After the above selection criteria being applied, the non- $\gamma_{\text{ISR}}\mu^+\mu^-$ background contribution is found to be negligible ($< 0.2\%$) from a study using the inclusive MC sample.

To quantitatively validate the description of the irreducible background, a two-dimensional fit to the $\mu^+\mu^-$ mass distribution ($M_{\mu^+\mu^-}$) and the distribution $|\cos\theta_\mu|$ is applied at control samples. In the fit, the shape of the background component is extracted from the corresponding simulated MC sample, and the shape of the signal comes from the simulation at 3.5080 GeV smeared with a Gaussian function to account for the resolution difference between different c.m. energies. The number of the signal component is expected to be zero in case of a perfect background MC simulation.

Non-zero N_{sig} is observed in the control sample at all c.m. energies, as summarized in Table I, representing a discrepancy between data and MC simulation of the background process. The significance is calculated by comparing the fit likelihoods with and without the signal. Then significance values are normalized to a typical size of the χ_{c1} scan sample of 180 pb^{-1} . The scaled significance values are found to be below 2.3σ .

This discrepancy cannot be explained by data-MC detection differences (*e.g.* tracking efficiency, etc.), but can be the limitation of the PHOKHARA generator in simulating narrow resonances. A two-dimensional correction is applied to correct for the discrepancy. The correction factors are extracted using data and MC samples at $\sqrt{s} = 3.773$ or 4.178 GeV and applied to MC simulations at other energy points. Using either correction factors, the N_{sig} at control samples are consistent with zero within one standard deviation, as shown in Table I.

TABLE I. The c.m. energies (\sqrt{s}), integrated luminosities (\mathcal{L}) and fit results of control samples (above the horizontal line) and of χ_{c1} scan sample (below). Fit is applied without (N_{sig} w/o Cor.) and with (N_{sig} w/ Cor.) the two-dimensional correction. The first uncertainty is statistical, and the second one is systematic (if applied). In each brackets, the first value denotes the statistical significance, and the second value denotes a normalization to 180 pb^{-1} (in case of control samples) and the significance including the systematic uncertainty (for the χ_{c1} scan sample). In the last column, the numbers are determined with the common fit to all χ_{c1} scan sample. At 3.5104 GeV, the negative significance means that after including the signal component, the goodness of agreement between data and MC get worse.

\sqrt{s} (MeV)	\mathcal{L} (pb^{-1})	N_{sig} w/o Cor.	N_{sig} w/ Cor.	N_{sig} w/ Cor. common fit
3773.0	2932.4	1097 ± 25 (7.6 σ ; 1.9 σ_{180})	47 ± 50 (0.3 σ ; 0.1 σ_{180})	–
4178.4	3192.5	544 ± 7 (5.0 σ ; 1.2 σ_{180})	18 ± 36 (0.2 σ ; 0.0 σ_{180})	–
3581.5	85.3	10 ± 1 (0.3 σ ; 0.4 σ_{180})	3 ± 6 (0.4 σ ; 0.6 σ_{180})	–
3670.2	83.6	43 ± 7 (1.6 σ ; 2.3 σ_{180})	7 ± 10 (0.2 σ ; 0.3 σ_{180})	–
3508.0	181.8	321 ± 21 (6.5 σ)	$210 \pm 15 \pm 18$ (4.1 σ ; 4.0 σ_{low})	191_{-59}^{+60} (4.5 σ ; 4.0 σ_{low})
3509.7	39.3	85 ± 28 (3.9 σ)	$63 \pm 27 \pm 6$ (2.8 σ ; 2.7 σ_{low})	41_{-19}^{+20} (2.4 σ ; 2.3 σ_{low})
3510.4	183.6	96 ± 95 (1.2 σ)	$0 \pm 62 \pm 26$ (0.1 σ ; 0.0 σ_{low})	42_{-77}^{+79} (–1.7 σ ; –2.5 σ_{low})
3514.6	40.9	-17 ± 1 (0.8 σ)	$-41 \pm 3 \pm 7$ (1.8 σ ; 1.6 σ_{low})	-29_{-10}^{+8} (1.6 σ ; 1.7 σ_{low})
Combined	445.6	–	(5.3 σ ; 5.1 σ_{low})	(5.1 σ ; 4.2 σ_{low})

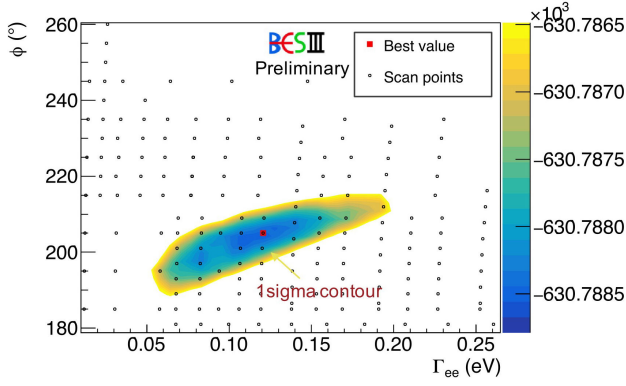


FIGURE 2. The contour of Γ_{ee} and ϕ at 68.3% C.L. on the distribution of $-\log(L)$. The black open circles are the parameter points with which the MC samples are produced. The red points represents the one where the likelihood value has a maximum.

At the χ_{c1} scan samples, the shapes of the contributions, *i.e.* the coherent sum of the amplitudes of the signal process and the irreducible background processes, depends on Γ_{ee} of χ_{c1} and the relative phase ϕ between signal and the ISR background. The two parameters have been predicted in Ref. [12]. However, they can be measured from data as well. We use a scan method to determine the values since getting an analytic formula of the total cross section of $e^+e^- \rightarrow \gamma_{\text{ISR}}\mu^+\mu^-$ as a function of Γ_{ee} and ϕ is not easily possible. The MC samples are produced at different values of (Γ_{ee}, ϕ) in the parameter space, shown as open circles in Fig. 2. At different (Γ_{ee}, ϕ) , the goodness of the agreement between data and MC samples are described via a log likelihood ($-\log L$) method taken from a two-dimensional fit (referred to as common fit). In the fit, four χ_{c1} scan samples are considered simultaneously, the number of events are constrained to the expected number of events calculated with corresponding cross section and integrated luminosity. At 68.3% C.L., the contour of Γ_{ee} and ϕ on the distribution of $-\log L$ is shown in Fig. 2. The best Γ_{ee} and ϕ parameters are determined to be 0.120 eV and 205.0°, respectively.

The number of signal events in the χ_{c1} scan sample obtained from the scan result are listed in Table I (N_{sig} w/

Cor. common fit). However, the result from the common fit is strongly constrained to the total cross section line-shape given by the theoretical calculation in Ref. [12]. To release the constraint that the Γ_{ee} and ϕ parameters should be exactly the same for the four χ_{c1} scan samples, two-dimensional fits are performed at each data sample individually (referred to as individual fit). In the fit, the numbers of χ_{c1} ($N_{\chi_{c1}}$) and background events (N_{bg}) are free parameters, the interference (N_{int}) is written as $f \cdot \sqrt{N_{\chi_{c1}} \cdot N_{\text{bg}}}$, where f is determined from the common fit and represents the dependence of N_{int} to $N_{\chi_{c1}}$ and N_{bg} . The line-shapes of the χ_{c1} production, the irreducible background, and the interference between them are extracted from the corresponding individual MC simulations. For the two-dimensional correction, it is applied on the shapes of background, and the square root of the same factor is used for the interference. Results from the individual fit method for $M_{\mu^+\mu^-}$ are shown in Fig. 3 and are listed in Table I. An excess of events is seen at $\sqrt{s} = 3.5080$ and 3.5097 GeV, with N_{sig} (statistical significance) determined to be 210 ± 15 (4.1σ) and 63 ± 27 (2.8σ), separately. The signal component is not significant at $\sqrt{s} = 3.5104$ GeV, which is determined to be 0 ± 62 (0.1σ). At $\sqrt{s} = 3.5146$ GeV, a reduction is seen with $N_{\text{sig}} = -41 \pm 3$ (1.8σ). The behaviour at the χ_{c1} scan sample is quantitatively in excellent agreement with the prediction of Ref. [12]. By combining the four χ_{c1} scan samples, the statistical significance of the process $e^+e^- \rightarrow \chi_{c1}$ is found to be 5.3σ .

Systematic uncertainties for the extraction of Γ_{ee} and ϕ mainly come from the luminosity measurement, the detection efficiency, the fit method, the two-dimensional correction, the non- $\gamma_{\text{ISR}}\mu^+\mu^-$ background contribution, and the c.m. energy measurement. The systematic uncertainty of the integrated luminosity is 0.6% for each data sample. The uncertainty in lepton reconstruction is included in the integrated luminosity measurement since we require two leptons in both selection criteria. The uncertainty in photon reconstruction is 1% [19]. The systematic uncertainties from the integrated luminosity measurement and the photon reconstruction are combined by changing the normalization factors used in the scan fit by 1%. The uncertainty from the selection applied

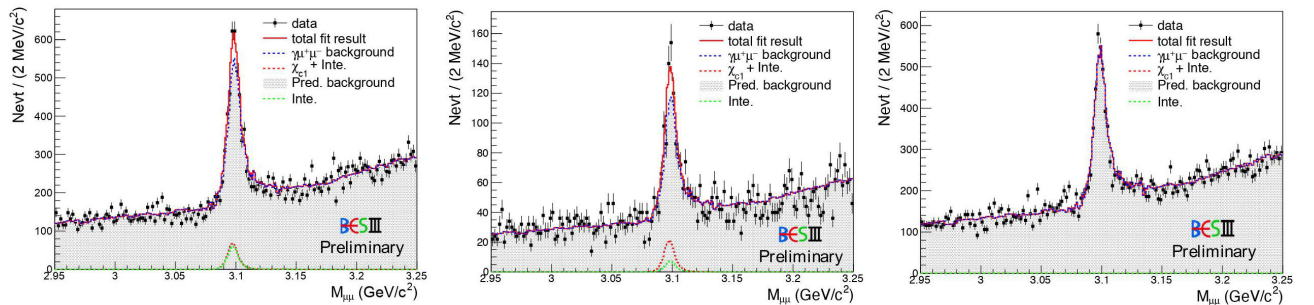


FIGURE 3. Individual fit result projecting on $M_{\mu^+\mu^-}$ at χ_{c1} scan sample. From left to right separately show distributions at 3.5080, 3.5097, 3.5104 and 3.5146 GeV. The dots with error bars are distributions from data, the red curve is the best fit result, the dashed red (blue, green) curve is signal (background, interference) contribution. The gray histogram is the predicted background normalized according to integrated luminosity.

on the polar angle of the photon is studied by tightening the requirement on $|\cos\theta_\gamma|$ from 0.8 to 0.79, 0.78, 0.77 and 0.76. The largest deviation with respect to the default angle cut is taken as the systematic uncertainty. The uncertainty from the binning is studied by simulating toy MC samples, no bias was found. With the help of the BEMS system, the beam energy spread is measured to be 736 ± 27 keV. The uncertainty from the MC line-shape introduced by the beam energy spread is considered by changing the beam-energy spread from 736 to 1000 keV, the change is much larger than one standard deviation. The uncertainty from the choice of the fit range is studied by systematically changing this fit range. In the nominal result, the two-dimensional correction factors are extract from the $\sqrt{s} = 3.773$ GeV data sample. It is replaced by that from the $\sqrt{s} = 4.178$ GeV data sample to estimate the systematic uncertainty. In addition, the square root of the two-dimensional correction is applied to the interference term based on the assumption that the discrepancy observed at control sample all comes from generator level. The uncertainty from this assumption is studied by dropping the correction to the interference term, the changes are taken as systematic uncertainty. The non- $\gamma_{\text{ISR}}\mu^+\mu^-$ background contribution is neglected in the nominal result. The uncertainty from it is considered by including it in the fit. The c.m. energy is measured with BEMS system with an uncertainty of ± 0.05 MeV. As the total cross section of $e^+e^- \rightarrow \gamma_{\text{ISR}}\mu^+\mu^-$ changes significantly only for the third point, we change the \sqrt{s} for the third point in MC simulation from 3.5104 to 3.5103 or 3.5105 GeV and take the changes

as systematic uncertainty. Assuming all the systematic uncertainties are uncorrelated and adding them in quadrature, Γ_{ee} and ϕ are determined to be $0.120_{-0.08}^{+0.13}$ eV and $205.0_{-22.4}^{+15.4}^\circ$, respectively.

For the individual fit, the systematic uncertainties are estimated similarly, but excluding these requirements where the statistic changes. There is one extra term coming from the input Γ_{ee} and ϕ values. This is considered by varying the values within the 68.3% C.L. contour.

4. Summary

In summary, using four data samples taken by the BESIII detector in the χ_{c1} mass region, we for the first time observe the direct production of the C -even resonance χ_{c1} in e^+e^- annihilation with a combined statistical significance of 5.3σ . We see an excess of J/ψ events at $\sqrt{s} = 3.5080, 3.5097$ GeV, and a reduction at $\sqrt{s} = 3.5146$ GeV. This observation agrees with the prediction of an interference effect between the direct process of $e^+e^- \rightarrow \chi_{c1} \rightarrow \gamma J/\psi \rightarrow \gamma\mu^+\mu^-$ and the ISR processes of $e^+e^- \rightarrow \gamma_{\text{ISR}}J/\psi \rightarrow \gamma_{\text{ISR}}\mu^+\mu^-$ and $e^+e^- \rightarrow \gamma_{\text{ISR}}\mu^+\mu^-$. The electronic width, Γ_{ee} , and the relative phase, ϕ , are determined to be $0.120_{-0.08}^{+0.13}$ eV and $205.0_{-22.4}^{+15.4}^\circ$, respectively. This research provides a new production method of C -even states (conventional or exotic) in e^+e^- experiments. Using future super-tau-charm factories with increased luminosity, the Γ_{ee} and other properties such as line-shape of C -even states could be determined similarly.

1. J. H. Kühn, J. Kaplan and E. G. O. Safiani, Electromagnetic Annihilation of e^+e^- Into Quarkonium States with Even Charge Conjugation, *Nucl. Phys. B* **157** (1979) 125; [https://doi.org/10.1016/0550-3213\(79\)90055-5](https://doi.org/10.1016/0550-3213(79)90055-5); J. Kaplan and J. H. Kühn, Direct Production of 1^{++} States in e^+e^- Annihilation, *Phys. Lett. B* **78** (1978) 252; [https://doi.org/10.1016/0370-2693\(78\)90017-5](https://doi.org/10.1016/0370-2693(78)90017-5).
2. P. V. Vorobev *et al.* (ND Collaboration), Upper limits of the electron widths of the C -even mesons $\eta(975)$, $f_2(1270)$, $f_0(1300)$, $a_0(980)$, and $a_2(1320)$, *Sov. J. Nucl. Phys.* **48** (1988) 273.
3. M. N. Achasov *et al.* (SND Collaboration), Search for direct production of $a(2)(1320)$ and $f(2)(1270)$ mesons in e^+e^- annihilation, *Phys. Lett. B* **492** (2000) 8; [https://doi.org/10.1016/S0370-2693\(00\)01090-X](https://doi.org/10.1016/S0370-2693(00)01090-X).
4. M. N. Achasov *et al.* (SND Collaboration), Search for the process $e^+e^- \rightarrow \eta$, *Phys. Rev. D* **98** (2018) 052007; <https://doi.org/10.1103/PhysRevD.98.052007>.
5. R. R. Akhmetshin *et al.* (CMD-3 Collaboration), Search for the process $e^+e^- \rightarrow \eta'(958)$ with the CMD-3 detector, *Phys. Lett. B* **740** (2015) 273; <https://doi.org/10.1016/j.physletb.2014.11.056>.
6. M. N. Achasov *et al.* (SND Collaboration), Search for the $\eta' \rightarrow e^+e^-$ decay with the SND detector, *Phys. Rev. D* **91** (2015) 092010; <https://doi.org/10.1103/PhysRevD.91.092010>.
7. M. N. Achasov *et al.* (SND Collaboration), Search for direct production of the $f_1(1285)$ resonance in e^+e^- collisions, *Phys. Lett. B* **800** (2020) 135074; <https://doi.org/10.1016/j.physletb.2019.135074>.
8. M. Ablikim *et al.* (BESIII Collaboration), An improved limit for Γ_{ee} of $X(3872)$ and Γ_{ee} measurement of $\psi(3686)$, *Phys. Lett. B* **749** (2015) 414; <https://doi.org/10.1016/j.physletb.2015.08.013>.
9. Y. Teramoto *et al.* (Belle Collaboration), Evidence for $X(3872) \rightarrow J/\psi\pi^+\pi^-$ Produced in Single-Tag Two-Photon Interactions, *Phys. Rev. Lett.* **126** (2021) 122001; <https://doi.org/10.1103/PhysRevLett.126.122001>.
10. A. Denig, F. K. Guo, C. Hanhart, and A. V. Nefediev, Direct $X(3872)$ production in e^+e^- collisions, *Phys. Lett. B* **736** (2014) 221; <https://doi.org/10.1016/j.physletb.2014.07.027>.
11. N. Kivel and M. Vanderhaeghen, $\chi_{cJ} \rightarrow e^+e^-$ decays revisited, *JHEP* **02** (2016) 032; [https://doi.org/10.1007/JHEP02\(2016\)032](https://doi.org/10.1007/JHEP02(2016)032).
12. H. Czyż, J. H. Kühn and S. Tracz, χ_{c1} and χ_{c2} production at e^+e^- colliders, *Phys. Rev. D* **94** (2016) 034033; <https://doi.org/10.1103/PhysRevD.94.034033>.

13. M. Ablikim *et al.* (BESIII Collaboration), Design and Construction of the BESIII Detector, *Nucl. Instrum. Meth. A* **614** (2010) 345, <https://doi.org/10.1016/j.nima.2009.12.050>.
14. C. H. Yu *et al.*, *BEPCII Performance and Beam Dynamics Studies on Luminosity*, Proceedings of IPAC2016, Busan, Korea, 2016. <https://doi.org/10.18429/JACoW-IPAC2016-TUYA01>.
15. J. Y. Zhang *et al.*, Upgrade of Beam Energy Measurement System at BEPC-II, *Chin. Phys. C* **40** (2016) 076001, <https://doi.org/10.1088/1674-1137/40/7/076001>.
16. S. Agostinelli *et al.* (GEANT4 Collaboration), GEANT4—a simulation toolkit, *Nucl. Instrum. Meth. A* **506** (2003) 250, [https://doi.org/10.1016/S0168-9002\(03\)01368-8](https://doi.org/10.1016/S0168-9002(03)01368-8).
17. H. Czyż, A. Grzebińska, and J. H. Kühn, Narrow resonances studies with the radiative return method, *Phys. Rev. D* **81** (2010) 094014, <https://doi.org/10.1103/PhysRevD.81.094014>.
18. M. Ablikim *et al.* (BESIII Collaboration), Measurement of $e^+e^- \rightarrow \gamma\chi_{c0,c1,c2}$ cross sections at center-of-mass energies between 3.77 and 4.60 GeV, *Phys. Rev. D* **104** (2021) 092001, <https://doi.org/10.1103/PhysRevD.104.092001>.
19. M. Ablikim *et al.* (BESIII Collaboration), Branching fraction measurements of χ_{c0} and χ_{c2} to $\pi^0\pi^0$ and $\eta\eta$, *Phys. Rev. D* **81** (2010) 052005, <https://doi.org/10.1103/PhysRevD.81.052005>.